AIChE

Microstructure–Property–Quality-Correlated Paint Design: An LMC-Based Approach

Jie Xiao and Yinlun Huang
Dept. of Chemical Engineering and Materials Science, Wayne State University, Detroit, MI 48202

DOI 10.1002/aic.11651
Published online December 4, 2008 in Wiley InterScience (www.interscience.wiley.com).

Paint is designed to offer various chemical and physical properties for surface protection, styling, and appearance. Nevertheless, the anticipated quality of the surface coating is frequently unsatisfactory, which is often attributed to paint formulation. As new demands on coating performance continuously emerge, paint formulation design becomes much more challenging than ever. It is recognized that paint design can be significantly improved with the help of advanced computational methods, as they can provide great freedom and control over the investigation of paint formulation through any number of in silico *experiments virtually under any application conditions. This article introduces a lattice Monte Carlo based computational methodology for paint formulation design. By this methodology and structural analysis techniques, a variety of correlations among paint material, curing condition, coating microstructure, and coating qualities can be generated, which are critical for the development of superior paint formulations. A comprehensive study on acrylic-melamine-based paint design and analysis demonstrates the methodological efficacy.* © 2008 American Institute of Chemical Engineers *AIChE J,* 55: 132–149, 2009
Keywords: Lattice Monte Carlo modeling, polymer network structure, film curing, paint design, coating quality

Introduction

Paint is a polymeric material formulated to have a variety of chemical and physical properties, which are necessary for the paint-based surface coating to demonstrate its desired properties in styling, appearance, and durability. It is known that a well-controlled paint application process is critical for achieving high coating quality.[1–3] Industrial practice has shown that, however, certain types of coating quality problems are attributed mainly to paint design. On the other hand, demands on new coating performance, such as self-cleaning and self-healing, have emerged, which further challenges paint formulation design.

Over the past decades, the approaches for paint design have changed very little, most of which are still trial and error based.[4] In a usual procedure, paint formulation is determined in lab. The paint is then applied to a small substrate. The resulting thin layer of wet paint is cured under a preset curing condition. The cured film then undergoes a number of mechanical, chemical, and thermal tests to evaluate the coating performance. The test results will be analyzed to determine the acceptance of the paint formulation. Note that because of the complexity of paint design and the limitations on experimental cost and time, to identify an optimal paint formulation is always a very challenging task. On the other hand, experimental tests mostly do not include examination of the formation of coating microstructures. Even if such microstructures were attainable, how to correlate them with paint formulation and property, paint application process, and coating performance would be mostly unknown. It is recognized that revealing the relationship between a microscale material structure and macroscale coating properties becomes increasingly critical in material design and application. This is especially true for paint development and utilization.

Correspondence concerning this article should be addressed to Y. Huang at yhuang@wayne.edu.

It is observed that computer simulation techniques have been widely used in material design and application, as computer simulation can offer various important advantages over experimental and theoretical research.[5] The *in silico* experimental approaches can provide great freedom and control over the investigation of material formulation and chemical and physical properties through any number of virtual experiments under any processing conditions that need to be studied. There is no doubt that computational paint design will become most attractive to the improvement of the understanding of new paint formulation.

It is worth noting that general polymer network formations have been extensively studied through Monte Carlo (MC) simulation.[6–8] The studies investigated the network structures quantifiable by their molecular weight distribution, gel fraction, and cycle rank. However, the known simulation studies do not consider molecular motion effects, which can introduce considerable errors, especially for the densely cross-linked systems (e.g., the thermoset resins in automotive paint).[9] To overcome this deficiency, lattice MC (LMC) simulation embedded by a bond fluctuation (BF) model was studied.[5,10–14] In those studies, the networks were constructed on a cubic lattice, and the network structural properties, such as elastic material fraction, soluble fraction, and the number of loops and pendent structures, were evaluated. However, the studied materials were restricted to monodispersed, end-linked polymers. Moreover, nonisothermal curing conditions, which are usual industrial practice, were not taken into account in simulation, and the curing dynamics were investigated in terms of MC steps, rather than real curing time. These further restricted the usage of the methodology in paint design.

For paint design, Bauer et al. indicated that the elastic material fraction as a network structural property was not sufficiently suitable for evaluating surface coating properties. The elastically effective cross-link density (EECD), however, could correlate closely to the physical measures of paint cure.[15–17] They then introduced an EECD evaluation approach by resorting to the Macosko and Miller (M&M) theory.[18,19] In their approach, no network structure is needed in EECD calculation. Although the approach is simple to use, the calculation may contain a noticeable error because the spatial effects are not considered and ring (loop) formation in the network is ignored.[9,17]

In this article, we will introduce a comprehensive microscale modeling and analysis methodology for paint formulation design and surface coating property prediction. By this methodology, which is resorted to LMC modeling and simulation, any paint formulation can be evaluated under any real industrial curing condition, and coating performance can be thoroughly investigated. This can enable the establishment of important correlations among paint formulation, curing condition, coating microstructure, and coating properties. The introduced methodology can be used to study the construction and analysis of polymer networks, where the distributions of polymer molecular weights and functional groups on polymer chains are all taken into account. Different from the known LMC simulation techniques, this methodology allows imposing curing conditions to the network formation process, which permits investigation of curing dynamics along the real curing time rather than MC steps. Furthermore, a new polymer network analysis method is described for evaluating the EECD by utilizing the information contained in the three dimensional (3D) polymer network structures.

In the following text, a general LMC simulation modeling approach will be first presented. Then, a comprehensive simulation methodology for generating polymer network structures of paint materials will be described. Succeedingly, a coating quality focused polymer network analysis approach will be delineated. After that, a comprehensive study on the design and analysis of an acrylic-melamine-based paint material will be illustrated to show the methodological efficacy.

General Simulation Modeling

To study paint formulation design via LMC, a simulation model must be created first. The model should describe how the polymer chains and the cross-linkers in the paint are placed and how they can move around in the defined simulation lattice. In this work, the BFmodel by Deutsch and Binder is adopted.[20,21] In applying the BF modeling method, the simulation lattice is defined to have $n_x \times n_y \times n_z$ unit cubes (see Figure 1), and the periodic boundary condition (PBC)[22] should be imposed to the lattice so that the resulting simulation can reflect the properties of the bulk material. In the lattice, each unit cube is called a (lattice) cell, which has eight vertices called (lattice) sites. A cell can be occupied by no more than one effective unit (EU), either an effective monomer or cross-linker, which is located only in all the eight sites of the cell; such a cell is called an occupied cell (see Figure 1). Otherwise, it is called an unoccupied cell.

Excluded volume restriction

LMC simulation should be conducted under the excluded volume restriction.[21] This means that if a cell is occupied by an EU, then its 26 surrounding cells in the space must be unoccupied to avoid any lattice site occupied by more than one EU. In this way, an excluded volume interaction between any pair of EUs can be feasibly taken into account in simulation.

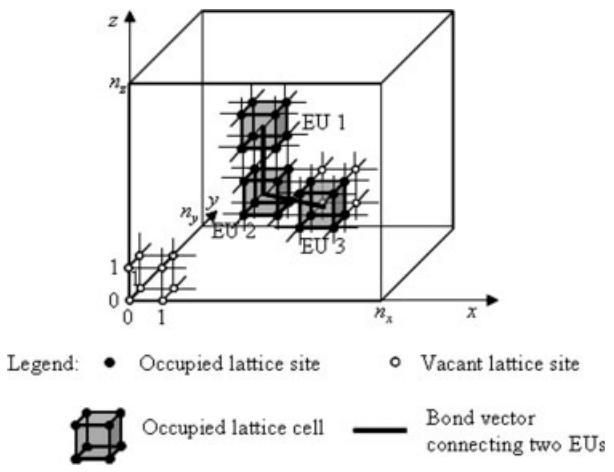

Figure 1. Sketch of a simulation lattice.

Permissible bond vectors

Each polymer chain is formed by connecting the centers of gravity of each pair of EUs. Note that the formed chains are not permitted to intersect each other when they move randomly; this allows the simulation of the entanglement restriction on polymer chain dynamics.[21] The restriction can be imposed by specifying a set of permissible bond vectors.[21] Note that a bond vector, denoted as $\omega = (\Delta x, \Delta y, \Delta z)$, shows a relative distance between two directly connected EUs. In Figure 1, for instance, the bond vector connecting EU 1 and EU 2 is (0, 0, 2) or (0, 0, −2), and the bond vector connecting EU 2 and EU 3 is (2, −1, 0) or (−2, 1, 0).

Taking the excluded volume restriction and the entanglement restriction into account, the feasible bond length, $\|\omega\|$, between the EUs can only be 2, $\sqrt{5}$, $\sqrt{6}$, 3, and $\sqrt{10}$.[21] Note that a bond shorter than 2 (i.e., $\sqrt{3}$, $\sqrt{2}$, 1 or 0) violates the excluded volume restriction. On the other hand, a bond longer than $\sqrt{10}$ may make the chains intersected.

Let Ω be a set of permissible bond vectors, each of which has one of the five bond lengths as listed earlier. This set contains a total of 108 bond vectors, which can be expressed as a union of six subsets as follows

$$\Omega = \Gamma(2,0,0) \cup \Gamma(2,1,0) \cup \Gamma(2,1,1) \cup \Gamma(2,2,1) \cup \Gamma(3,0,0) \cup \Gamma(3,1,0) \quad (1)$$

where Γ $(\Delta x, \Delta y, \Delta z)$ is a set of bond vectors that can be derived through performing a complete permutation of Δx, Δy, and Δz with sign changes. For instance, Γ(2, 1, 0) contains the following 24 bond vectors:

$$\begin{aligned}\Gamma(2,1,0) = \{&(2,1,0),\ (2,0,1),\ (0,2,1),\ (0,1,2),\ (1,2,0),\\ &(1,0,2),(-2,1,0),\ (-2,0,1),\ (0,-2,1),\\ &(0,1,-2),\ (1,-2,0),(1,0,-2),(2,-1,0),\\ &(2,0,-1),\ (0,2,-1),\ (0,-1,2),\ (-1,2,0),\\ &(-1,0,2),(-2,-1,0),\ (-2,0,-1),(0,-2,-1),\\ &(0,-1,-2),\ (-1,-2,0),(-1,0,-2)\}\end{aligned} \quad (2)$$

Note that Γ's contain different numbers of bond vectors. Also note that there is no subset Γ(2, 2, 0) because the length of each bond vector in this subset is $2\sqrt{2}$, which may cause chain intersection.[21]

EU movement feasibility

EUs can move continuously in the lattice, which mimics the random motion of polymer chains during coating curing in real paint application. The movement of the EUs can be simulated by their random hops.[13] In each simulation step, a randomly selected EU can be displaced, in an arbitrary direction, to a neighboring cell at one cell distance from its original location. That is, a relative position of the selected EU before and after a move must be in the set Γ(1, 0, 0) [i.e., one of the following vectors, (1, 0, 0), (0, 1, 0), (0, 0, 1), (−1, 0, 0), (0, −1, 0), (0, 0, −1)]. Note that a move is feasible only if it follows the excluded volume restriction and the resulting new bond vectors belong to set Ω.

The simulation model described earlier is a coarse-grained model. This is because each EU in the lattice is intended to mimic only the space-filling characteristics of a collection of atoms, for which no atomic details is involved explicitly.[23]

Polymer Network Formation Simulation Methodology

Paint usually is composed of resin, pigment, solvent, and additives. Investigation of paint performance by considering all four components simultaneously is extremely challenging. As the first step toward a complete paint design, this work studies the methodology for resin design. In paint, resin is used to bind the ingredients and to form the film. Paint coatings are often named after the resin, which consists of precursor polymer chains and cross-linker molecules. The formation of a polymer network can be simulated by following the steps below: (i) to set up a simulation system, (ii) to generate an initial configuration, (iii) to establish an equilibrium state, and (iv) to develop a polymer network. Note that the PBC[22] must be imposed in simulation so that the simulation result of a system containing a limited number of molecules can be used to characterize a coating layer on a substrate. In this section, a number of procedures for accomplishing the tasks are introduced in detail.

System set-up

Creation of precursor polymer chains and cross-linker molecules and determination of lattice size are the major tasks for simulation system set-up. Note that a study on the network of paint material requires considering the distributions of polymer molecular weight and functional groups. This is very different from the study of the network formed by monodispersed end-linked polymer.[5,12,13]

Precursor Polymer Chain Creation. The precursor polymers studied in this work are generated through random copolymerization and have a polydispersity index (PDI) value of around two. For such materials, it is reasonable to assume that the molecular weight distribution follows a most probable distribution, and the functional groups are randomly distributed in precursor polymer chains.[15] With these assumptions, the precursor polymer chains showing such characteristics can be created, and the number of precursor polymer chains (N_{pc}^{i}) having different chain lengths can be determined by,[24]

$$N_{\mathrm{pc}}^{i} = \mathrm{int}\left(N_{\mathrm{m}}^{\mathrm{set}} p^{(i-1)}(1-p)^2\right) \qquad i = 1, 2, \cdots \quad (3)$$

where $N_{\mathrm{m}}^{\mathrm{set}}$ is the prespecified total number of the effective monomers; i is the chain length quantified by the number of the effective monomers in a polymer chain; p is the polymerization conversion (between 0 and 1), which can be evaluated as:

$$p = 1 - \frac{M_{\mathrm{m}}}{\overline{M}_{\mathrm{n}}} \quad (4)$$

where M_{m} is the molecular weight of an effective monomer and $\overline{M}_{\mathrm{n}}$ is the polymer number average molecular weight. Note that the polymerization reaction leads to a creation of precursor polymer chains, whereas the cross-linking reaction

gives rise to the formation of a polymer network. These two types of reactions do not occur simultaneously. Based on Eq. 3, the total number of precursor polymer chains (N_p) and the total number of effective monomers (N_m) created for simulation can be expressed as:

$$N_p = \sum_{i=1}^{\infty} N_{pc}^i \tag{5}$$

$$N_m = \sum_{i=1}^{\infty} i N_{pc}^i \tag{6}$$

As the precursor polymer chains are linear, and a linear chain of length i contains $i - 1$ bonds, the total number of the initial bonds in the system is the difference between N_m and N_p, i.e.,

$$N_b^0 = \sum_{i}^{\infty} (i-1) N_{pc}^i \tag{7}$$

In this work, the functional groups involved are divided into two types: Type A that is in a precursor polymer chain and Type B that is in a cross-linker molecule. The initial total number of Type A functional groups (N_A^0) in the resin can be evaluated by:

$$N_A^0 = \text{int}\left(\frac{N_m M_m + N_c M_c}{M_A^{eq}}\right) \tag{8}$$

where M_c is the molecular weight of a cross-linker molecule; N_c the number of cross-linker molecules; M_A^{eq} the weight of the resin per mole of Type A functional group. Note that in the above equation, the numerator divided by the Avogadro constant is the total weight of the resin. Also note that in distributing randomly the functional groups to the effective monomers, each effective monomer has the same probability to contain one functional group.

Cross-linker Molecule Creation. If the ratio of the number of Type B to that of Type A functional groups (r_{BA}) is given, then the number of Type B functional groups (N_B^0) can be readily obtained, i.e.,

$$N_B^0 = \text{int}\left(r_{BA} N_A^0\right) \tag{9}$$

Assume that the functionality of a cross-linker molecule is f_c, which means that each cross-linker molecule contains f_c Type B functional groups ($f_c \geq 3$ in this work). The number of cross-linker molecules (N_c) can then be determined by:

$$N_c = \text{int}\left(\frac{N_B^0}{f_c}\right) \tag{10}$$

Lattice Size Determination. A lattice simulation system contains N_m effective monomers (indexed from 1 to N_m) and N_c cross-linkers (indexed from $N_m + 1$ to $N_m + N_c$). The size of a simulation lattice should be designed properly so that it can not only accommodate the $N_m + N_c$ EUs, but also allow them to move around during a relaxation process as well as during cross-linking reaction. To determine the lattice size, the volume fraction of polymer chains and cross-linker molecules needs to be given, usually around 0.45, which can be expressed as,[13]

$$\phi = \frac{8v(N_m + N_c)}{V} \tag{11}$$

where v is the volume of each lattice site in a (lattice) cell; V is the volume of all the sites in the lattice. Let n_x, n_y, and n_z be the number of cells in the x, y, and z coordinates, respectively. Then, the volume of all the sites in the lattice can be expressed as,

$$V = v(n_x + 1)(n_y + 1)(n_z + 1) \tag{12}$$

Usually, a regular cubic lattice (i.e., $n_x = n_y = n_z$) is selected for simulation. Hence, the number of cells in each coordinate of the simulation lattice becomes,

$$n_x = \text{int}\left(\left(\frac{8(N_m + N_c)}{\phi}\right)^{\frac{1}{3}} - 1\right) \tag{13}$$

Simulation Information Handling. Various types of information will be generated during simulation, which should be stored properly for easy utilization. In this work, five matrices are defined for this purpose.

(a) Lattice cell occupation matrix $\boldsymbol{L}_{n_x \times n_y \times n_z}$: The 3D matrix is used to record the cell occupation information. If cell (i, j, k) in the lattice is occupied by an EU whose index is I_{eu}, then element $l_{i,j,k}$ in L is set to I_{eu}; otherwise, it is set to 0. For a simulation system containing $N_m + N_c$ EUs, only $N_m + N_c$ elements in matrix $\boldsymbol{L}$ have nonzero values.

(b) EU location matrix $\boldsymbol{U}_{(N_m+N_c)\times 3}$: The cell occupation information contained in matrix $\boldsymbol{L}$ should be converted to the information of EU locations in the lattice. Hence, matrix $\boldsymbol{U}$ is introduced, in which each row gives a location vector. That is, vector ($u_{i,1}$, $u_{i,2}$, $u_{i,3}$) gives the location of the i-th EU.

(c) EU functionality vector $\boldsymbol{F}_{(N_m+N_c)\times 1}$: Each EU appeared in matrix $\boldsymbol{L}$ and listed in matrix $\boldsymbol{U}$ contains a certain number of functional groups. This information is listed in vector $\boldsymbol{F}$, whose row number is coincident with the row number of matrix $\boldsymbol{U}$, referring to the index assigned to each individual EU. For example, f_i gives the quantity of the functional groups belonging to the i-th EU, whose location in the lattice is given by ($u_{i,1}$, $u_{i,2}$, $u_{i,3}$) in matrix $\boldsymbol{U}$.

(d) Bond matrix $\boldsymbol{B}_{N_b\times 2}$: A bond connects two EUs. The bond information is recorded in $\boldsymbol{B}$. For instance, elements $b_{i,1}$ and $b_{i,2}$ give the index numbers of the two EUs that are connected by the i-th bond. Different from matrices $\boldsymbol{L}$ and $\boldsymbol{U}$ and vector $\boldsymbol{F}$ introduced above, the number of rows of matrix $\boldsymbol{B}$ will be continuously increased from N_b^0 to N_b^0 + min [N_A^0, N_B^0], as the number of bonds is increased during cross-linking reaction.

(e) EU connection matrix $\boldsymbol{G}_{(N_m+N_c)\times f_c}$: For a linear polymer chain, an effective monomer can be connected to no more than two effective monomers. Moreover, because each effective monomer has at most one functional group, it can be connected to no more than one cross-linker if a reaction takes place between them. For each cross-linker, the number of effective monomers it can connect depends on its functionality ($f_c \geq 3$). The connection information is stored in matrix $\boldsymbol{G}$, where $g_{i,j}$ gives the index number of the EU that is

connected to the i-th EU. For instance, if the i-th EU connects with three other EUs (j-th, k-th, and l-th), then the first three elements in the i-th row of matrix $\boldsymbol{G}$ are of the values of j, k, and l, and the remaining elements are set to 0.

Initial configuration generation

The simulation requires setting up an initial system configuration where EUs are properly placed in the lattice. The initial configuration can be created through placing all the molecules, including N_p polymer chains (i.e., N_m effective monomers connected by N_b^0 bonds) and N_c cross-linkers, without violating the excluded volume restriction and the bond vectors feasibility. The placement of the polymer chains and the cross-linkers can be accomplished by (i) generating a queue of polymer chains according to their lengths (with the longest one first, and the molecules of individual effective monomers and cross-linkers not involved in any chain are in the end) and (ii) placing the molecules in the queue one by one into the lattice by following the steps below. Again, each placement must satisfy the excluded volume restriction.

Step 1. Place the first EU of the chain in the queue to a randomly selected unoccupied lattice cell. Accordingly, this cell occupation information is recorded in matrices $\boldsymbol{L}$ and $\boldsymbol{U}$.

Step 2. Identify the next EU of the chain in the queue and place it to an unoccupied lattice cell based on a randomly selected bond vector ω in set Ω. Correspondingly, matrices $\boldsymbol{L}$ and $\boldsymbol{U}$ are updated. Then, go to *Step 4*. On the other hand, if no feasible unoccupied lattice cell is identified to place the EU after a certain number of attempts, then go to *Step 3*.

Step 3. Place the current EU back to the queue and also remove the most recently placed EU in the lattice back to the queue. Accordingly, matrices $\boldsymbol{L}$ and $\boldsymbol{U}$ need to be changed back. Then, return to *Step 2*.

Step 4. Check if the chain has any EU left for placement. If yes, return to *Step 2*; otherwise, continue.

Step 5. Check if any chain in the queue has not been placed. If yes, return to *Step 1*; otherwise, continue.

Step 6. Place all the individual EUs left in the queue to a feasible unoccupied cell and update matrices $\boldsymbol{L}$ and $\boldsymbol{U}$. This step continues until all the individual EUs are properly placed in the lattice.

Step 7. Output matrices $\boldsymbol{L}$ and $\boldsymbol{U}$ that contain the complete information of the initial configuration.

Equilibrium state creation

The initial system needs to be relaxed athermally to reach an equilibrium state.[5,13,23] The system is deemed to be in an equilibrium state when the mean squared displacements of the individual effective monomers and cross-linkers, and the mean squared position change of the center of gravity of the precursor polymer chains are not less than a half of the simulation lattice length.[5] This can be achieved by moving EUs in a stochastic way through a sufficiently large number of MC steps (e.g., $10^6 \sim 10^9$ steps, depending on the number of EUs involved in simulation).[5,12,13,23] The following procedure is designed for this purpose.

Step 1. Initiate a new MC step by selecting randomly an EU from matrix $\boldsymbol{U}$. Note that for the i-th EU selected, its location in the lattice is contained in the i-th row of matrix $\boldsymbol{U}$, i.e., vector $\boldsymbol{u}_i$ (or ($u_{i,1}$, $u_{i,2}$, $u_{i,3}$)).

Step 2. Determine a new position for the EU to move through randomly selecting a vector from set Γ (1,0,0), e.g., γ_j. The new position is given by vector $\boldsymbol{u}_i + \gamma_j$.

Step 3. Move the EU to the new position and update matrices $\boldsymbol{L}$ and $\boldsymbol{U}$, if the move does not violate the excluded volume restriction and the resulting new bond vectors are in set Ω. Otherwise, this move attempt must be discarded.

Step 4. Check if the number of MC steps has reached the preset maximum number. If no, return to *Step 1*; otherwise, the relaxation process is finished.

By combining the information contained in matrices $\boldsymbol{G}$ and $\boldsymbol{U}$, the bonds affected by the EU displacement as well as the new bond vectors can be readily determined. It should be pointed out that no EU displacement involves chemical reaction. Therefore, there is no new bond created in this process. Obviously, matrices $\boldsymbol{F}$, $\boldsymbol{B}$, and $\boldsymbol{G}$ keep unchanged in this process.

Polymer network formation

After the system reaches an equilibrium state which is defined in the preceding section, polymer networks can be formed through cross-linking reactions and the system leaves the original equilibrium state. The reactions are initiated when the paint film is baked at an adequate curing environment. The known studies on curing dynamics during polymer network formation were presented solely by either a number of prespecified MC steps or a reaction conversion,[5,12,13] where no nonisothermal curing condition was imposed. To ensure a full realization of the anticipated coating properties by the designed paint material, a practical curing condition, which gives a coating layer an adequate thermal profile, must be imposed in simulation, and the number of MC steps for simulation must be correlated to the prespecified curing time.

Curing Condition Imposing and Curing Time-MC Step Conversion. The rate of cross-linking reaction during film curing can be expressed as follows[25]:

$$\frac{d\alpha}{dt} = \zeta \exp\left(\frac{-E}{RT}\right)(1-\alpha)^n \tag{14}$$

where α is the conversion of a functional group; n the order of reaction; ζ the temperature-independent frequency factor; E the activation energy; R the gas constant; T the curing temperature; t the curing time.

For nonisothermal curing, if the required curing time is divided into a sufficiently large number of time intervals, then in each interval, the curing temperature, $T(t)$, can be safely treated as a constant. Equation 14 can then be applied to each time interval, and an integration of the equation gives:

$$\int_{\alpha_{i-1}}^{\alpha_i} \frac{1}{(1-\alpha)^n} d\alpha = \zeta \exp\left(\frac{-E}{RT_{i-1}}\right) \times \int_{t_{i-1}}^{t_i} dt \quad i = 1, 2, \cdots, I_{\max} \tag{15}$$

where α_i (i.e., $\alpha(t_i)$) and T_i (i.e., $T(t_i)$) are, respectively, the conversion and the curing temperature at the i-th time instant (t_i). $I_{\max}$ is the total number of time intervals, which is equal to the total number of time steps. Solving the above equation gives:

$$\Delta t_i = \begin{cases} \frac{1}{\zeta}\ln\left(\frac{1-\alpha_{i-1}}{1-\alpha_i}\right)\exp\left(\frac{E}{RT_{i-1}}\right), & \text{if } n=1 \\ \frac{(1-\alpha_{i-1})^{1-n}-(1-\alpha_i)^{1-n}}{\zeta(1-n)}\exp\left(\frac{E}{RT_{i-1}}\right), & \text{if } n>1 \end{cases} \quad i=1,2,\cdots,I_{\max} \tag{16}$$

and

$$\alpha_i = \alpha_{i-1} + \frac{N_A(t_{i-1}) - N_A(t_i)}{N_A^0} \qquad i=1,2,\cdots,I_{\max} \tag{17}$$

where $N_A(t_i)$ is the number of Type A functional groups at t_i.

The time instant in curing can be considered as an initiation of a new MC step when simulating a curing operation. Thus, a curing operation through $I_{\max}$ time steps can be simulated through $I_{\max}$ MC steps. Note that according to Eq. 16, the curing temperatures applied to the film in different curing time intervals are different. Hence, the lengths of the individual time intervals may be different. Furthermore, the total number of time steps can be determined only during curing operation simulation. Note that after the i-th MC step (i = 1, 2,. . ., $I_{\max}$), the number of Type A functional groups ($N_A(t_i)$) is recorded in EU functionality vector $\boldsymbol{F}$. This information will be used to calculate the cross-linking conversion (α_i) as well as the length of the i-th time interval (Δt_i). The accumulative curing time will be checked to ensure that the curing operation will be under control through terminating the MC simulation.

Network Formation Procedure. The simulation for network formation should be performed by allowing EUs with different types of functional groups to move randomly to the nearest distance and to react among them under a specific curing condition; such a phenomenon should be continued until a preset curing operation is finished. The simulation can be accomplished by following the procedure below.

Step 1. Initialize the simulation by setting the index (i), the cross-linking reaction conversion (α_i), and the total elapsed reaction time ($t_{\text{spent}}^{\text{curing}}$) each to 0; set the initial film temperature ($T(0)$) to T_0, and then input the required total curing time ($t_{\max}^{\text{curing}}$) and the desired curing temperature profile ($T(t)$, $0 \le t \le t_{\max}^{\text{curing}}$).

Step 2. Start a new simulation step by setting $i = i + 1$

Step 3. Conduct a move attempt for a randomly selected EU by following the substeps below.

Step 3-1. Select randomly an EU from matrix $\boldsymbol{U}$. Note that for the j-th EU selected, its location in the lattice is contained in the j-th row of matrix $\boldsymbol{U}$, i.e., vector $\boldsymbol{u}_j$ (or ($u_{j,1}$, $u_{j,2}$, $u_{j,3}$)).

Step 3-2. Determine a new position for the EU to move through randomly selecting a vector from set Γ (1,0,0), e.g., γ_k. The new position is given by vector $\boldsymbol{u}_j + \gamma_k$.

Step 3-3. Move the EU to the new position and update matrices $\boldsymbol{L}$ and $\boldsymbol{U}$, if the move does not violate the excluded volume restriction and the resulting new bond vectors are in set Ω. Otherwise, this move attempt must be discarded.

Step 4. Perform cross-linking reactions between the selected EU with other EUs by following the substeps below.

Step 4-1. Check if there is a remaining functional group on this EU. If yes, continue; otherwise, go to *Step 5*.

Step 4-2. Check if there is a neighboring EU located in two lattice cell distance from it (i.e., its relative position to the selected EU is in set Γ(2,0,0)); this neighboring EU must have a different type of functional groups and also have at least one remaining functional group for reaction. If not all these conditions are met, go to *Step 5*; otherwise create a bond between the selected EU and the neighboring EU to signify a reaction between them. Correspondingly, matrices $\boldsymbol{F}$, $\boldsymbol{B}$, and $\boldsymbol{G}$ should be updated due to this reaction.

Step 4-3. Return to *Step 4-1* for another possible bond creation.

Step 5. Obtain $N_A(t_i)$ from matrix $\boldsymbol{F}$ and then calculate cross-linking conversion α_i according to Eq. 17.

Step 6. Use the film temperature T_{i-1} and the calculated α_i to calculate Δt_i according to Eq. 16.

Step 7. Update the spent curing time by using $t_{\text{spent}}^{\text{curing}} = t_{\text{spent}}^{\text{curing}} + \Delta t_i$, and obtain film temperature T_i.

Step 8. Check if $t_{\text{spent}}^{\text{curing}} \le t_{\max}^{\text{curing}}$ or not. If yes, return to *Step 2*; otherwise, terminate the simulation as the network formation is accomplished.

Polymeric Network Analysis and Coating Quality Evaluation

According to Flory (1953), a polymer is soluble in a suitable solvent before the gel point. At the gel point, the film transforms suddenly from a viscous liquid to an elastic gel. Beyond the gel point, it is no longer fusible to a liquid nor is it entirely soluble in solvents. Naturally, these characteristics (gelation and attendant insolubility) are attributed to the restraining effects of the 3D network structures of an infinite size within the polymer.[24] This infinitely sized network is a gel, which must be the largest molecule in the system.

The simulation for network formation can generate possibly many networks of different sizes. The largest network must be identified because the coating quality largely depends on its structural property; it is named the INF network in this work. This network needs to be identified continuously throughout the curing process. Note that the INF network before the formation of the gel is the largest molecule in the system, but not a network of infinite size yet.

Many approaches are available for analyzing the structural properties of polymeric networks,[5,13,26,27] which can be used to, for example, determine the soluble material fraction and identify the types of network defects, such as pendent structures and loops. However, the available approaches are limited to the system with end-linked polymer networks, where a precursor polymer chain can only have two functional groups and they must be at its both ends. Note that for the

paint material, a precursor polymer chain can have more than two functional groups and the distribution of the functional groups in each chain is random. This structural complexity makes network identification and analysis very challenging. Moreover, the available approaches are for determining the fractions of elastic material, soluble material, pendent material, and loops. These structural properties are not directly correlated to paint-based coating properties of interest. This renders a need for identifying new types of structural properties that should be obtainable from the 3D polymer networks.

Elastically effective cross-link density

The EECD has been proven experimentally to be a very suitable indicator of the structural performance of a network, as it correlates well to certain coating physical and chemical properties.[15–17] In this work, we introduce an approach for evaluating the EECD of a film based on the information extracted from the 3D INF network that is formed during film curing.

The EECD is the number of moles of the elastically effective network chains (EENCs) per unit weight of a coating sample.[15] For the simulation system studied in this work, the number of EENC ($N_{\mathrm{EENC}}(t)$) changes along the curing time, so does the EECD. The following gives a formula for estimating the EECD.

$$\mathrm{EECD}(t) = \frac{N_{\mathrm{EENC}}(t)}{N_{\mathrm{m}}M_{\mathrm{m}} + N_{\mathrm{c}}M_{\mathrm{c}} - (N_{\mathrm{b}}(t) - N_{\mathrm{b}}^{0})M_{\mathrm{bp}}} \tag{18}$$

Note that $N_{\mathrm{EENC}}(t)$ divided by the Avogadro constant is the number of moles of EENCs at time t. The denominator of the right side of Eq. 18 divided by the Avogadro constant is the total weight of the coating sample. Note that the term, $N_{\mathrm{b}}(t) - N_{\mathrm{b}}^{0}$, gives the number of the bonds generated during cross-linking reactions. Each bond represents one reaction, and each reaction generates one by-product molecule with the molecular weight of M_{bp}. Hence, the term, $(N_{\mathrm{b}}(t) - N_{\mathrm{b}}^{0})M_{\mathrm{bp}}$, divided by the Avogadro constant is the weight of the by-product. As the by-product is usually volatile, its weight should be deducted from the total weight of the coating sample.

It is clear that to estimate EECD(t), it is necessary to obtain $N_{\mathrm{b}}(t)$ and $N_{\mathrm{EENC}}(t)$. Note that $N_{\mathrm{b}}(t)$ is available in matrix $\boldsymbol{B}$ that is updated during simulation. The information of $N_{\mathrm{EENC}}(t)$ can be obtained from the 3D coating microstructure by following three major steps: (i) to identify the INF network (i.e., the largest molecule) of the simulated coating sample, (ii) to identify the elastically effective junctions and their connections in the network, and (iii) to evaluate $N_{\mathrm{EENC}}(t)$. The major steps are delineated in the following sections.

Network identification

During curing, when the gel point appears, a polymer network of infinite size within the film starts to form. The coating system then contains two types of materials: a gel and a sol. The gel is the network portion (called the INF network) of the coating sample, which is the largest molecule containing the most EUs that are connected by bonds. The sol is the remaining structure that is not connected with the INF network.

The INF network can be identified by utilizing the information contained in bond matrix $\boldsymbol{B}$, where all the EUs linked by bonds are recorded. The information in this matrix needs to be converted and entered into a new vector, named molecule index vector $\boldsymbol{D}$, which has a dimension of $(N_{\mathrm{m}} + N_{\mathrm{c}}) \times 1$. The information extraction and conversion can be accomplished by following the procedure below.

Step 1. Initialize the molecule index, I_{mol}, to 0, and assign 0 to all the $N_{\mathrm{m}} + N_{\mathrm{c}}$ elements in vector $\boldsymbol{D}$, meaning that all the EUs have the same initial molecule index of 0.

Step 2. Obtain the index numbers of the two EUs, e.g., $b_{i,1}$ and $b_{i,2}$, from the top row of the remaining unchecked rows of matrix $\boldsymbol{B}$.

Step 3. Check the molecule index numbers of the two EUs in the $b_{i,1}$-th and $b_{i,2}$-th elements of vector $\boldsymbol{D}$, and then apply a suitable rule listed below to generate a molecule index number for both EUs and enter this number to the $b_{i,1}$-th, the $b_{i,2}$-th, and possibly other relevant elements of vector $\boldsymbol{D}$.

- Rule 1. If the $b_{i,1}$-th and $b_{i,2}$-th elements of vector $\boldsymbol{D}$ have a value of 0, then update the molecule index by using $I_{\mathrm{mol}} = I_{\mathrm{mol}} + 1$, and then enter I_{mol} into both elements.
- Rule 2. If one of the $b_{i,1}$-th and $b_{i,2}$-th elements of vector $\boldsymbol{D}$ has a nonzero value and the other one has a value of 0, then assign this nonzero value to the other element, meaning that the two corresponding EUs have the same molecule index.
- Rule 3. If the $b_{i,1}$-th and $b_{i,2}$-th elements of vector $\boldsymbol{D}$ have already had the same molecule index, then keep this index unchanged.
- Rule 4. If the $b_{i,1}$-th and $b_{i,2}$-th elements of vector $\boldsymbol{D}$ have two different nonzero values, then identify all the other elements in this vector that have the value the same as the larger value. After that, assign the smaller value for the $b_{i,1}$-th, the $b_{i,2}$-th, and all the identified elements in vector $\boldsymbol{D}$.

Step 4. Check if any bond in vector $\boldsymbol{B}$ has not been checked. If yes, return to *Step 2*; otherwise, continue.

Step 5. Check all the element values in vector $\boldsymbol{D}$. The nonzero number that appears most frequently gives the molecule that contains the most EUs. This number is named $I_{\mathrm{mol}}^{\max}$, and this molecule is the INF network.-

Step 6. Check each element in vector $\boldsymbol{D}$. If the i-th element is not equal to $I_{\mathrm{mol}}^{\max}$, which means that the i-th EU does not belong to the INF network, then all elements in the i-th row of matrix $\boldsymbol{G}$ will be set to 0. In the end, matrix $\boldsymbol{G}$ contains the connection information for the INF network only.

Note that after executing the procedure from Step 1 to Step 5, those EUs with the molecule index of 0 are individual effective monomers or cross-linkers; the EUs with nonzero molecule indices other than $I_{\mathrm{mol}}^{\max}$ belong to small molecules.

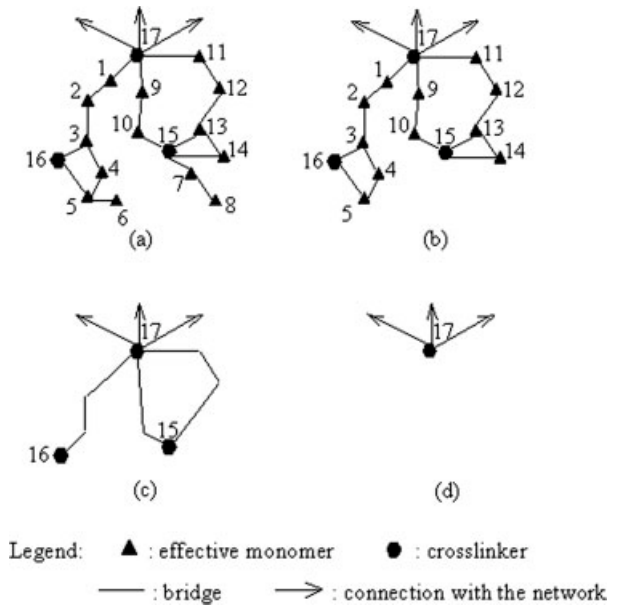

Figure 2. Stepwise illustration of identification of an elastically effective junction in Example 1.

Identification of elastically effective junctions and their connections

The identified INF network contains a very large number of chains. Each chain has two ends; each end is occupied by one EU. An end is called a terminal (point) if the EU connects to only one other EU by a bridge or bridges; otherwise, it is called a junction (point). A bridge is a direct connection between two EUs. A junction is elastically effective if the EU occupying it has at least three independent paths leading away to the INF network; otherwise, it is elastically ineffective.[28] The EUs not in either end of a chain are called divalent points.

Miller and Macosko stated that a network chain is elastically effective, if it is long and its both ends are elastically effective junctions (or cross-links).[18] Thus, the elastically effective network chains (EENCs) can be known by first identifying all the elastically effective junction points (EEJPs) and their connections. This can be readily accomplished by identifying and then excluding all those elastically ineffective junctions as well as those terminals in the network. The following procedure is designed for this purpose.

Step 1. Eliminate the terminal points and the associated bridges one by one by following the two substeps below.

Step 1.1. Delete an identified terminal point and the bridge(s) linking it to another EU. Check every row in matrix $\boldsymbol{G}$. If the i-th row contains only one nonzero index, e.g., j, which means that the i-th EU is a terminal point and it is connected to the j-th EU, then replace the index j in the i-th row by 0 and the index i in the j-th row also by 0.

Step 1.2 Check if any new terminal point is generated from the last step or if any terminal point is still left. If yes, return to *Step 1.1*; otherwise, go to *Step 2*.

Step 2. Replace the divalent points and the associated bridges one by one by following the substeps below.

Step 2.1. Delete an identified divalent point and the associated bridges linking it to two other EUs, and create a new bridge between these two EUs. Check every row in matrix $\boldsymbol{G}$. If the i-th row has two different nonzero indices, e.g., j and k, which means that the i-th EU is a divalent point and it is connected to the j-th and the k-th EUs, then clear the i-th row (i.e., set all elements to 0), replace (i) index i listed in the j-th row and in the k-th row by 0, and (ii) the number, 0, in the k-th row by index j and (iii) the number, 0, in the j-th row by index k.

Step 2.2. Check if any new divalent point is generated from the last step or if any divalent point is still left. If yes, return to *Step 2.1*; otherwise, go to *Step 3*.

Step 3. Check if any new terminal point is created in *Step 2*. If yes, return to *Step 1*; otherwise, stop. The INF network resulted through executing the above procedure is called a "reduced" network.

As a result of the above procedure, the connection information for the reduced network is stored in matrix $\boldsymbol{G}$. An application of the procedure above is illustrated by the two examples below.

Example 1. The initial structure in Figure 2a contains 17 EU's [including 14 effective monomers (No. 1–14) and three cross-linkers (No. 15–17)]. As shown, any path from EU 1, EU 2,. . ., or EU 16 to the INF network must go through EU 17. This means that each of the 16 EUs has only one path leading away to the INF network. Thus, they form a pendent structure. This pendent structure must be deleted from the network by executing the above procedure. Figures 2b, c give the intermediate results after implementing Steps 1 and 2 in the first round, whereas Figure 2d shows the final result

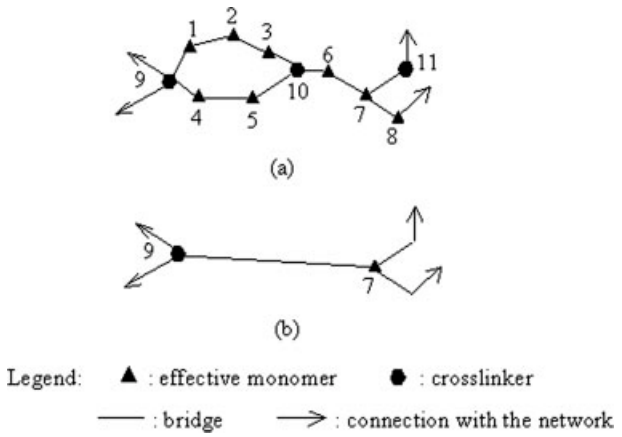

Figure 3. Stepwise illustration of identification of elastically effective junctions and their connections in Example 2.

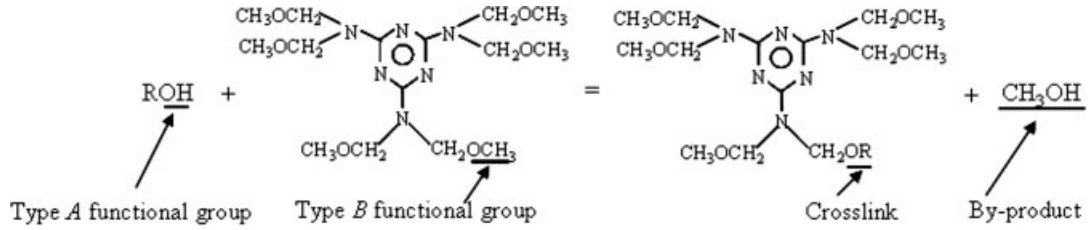

Figure 4. Crosslinking reaction formula for the acrylic-melamine coating formation.

after running the procedure in the second round. Note that in implementing the procedure, some EUs may change their types. For instance, EU 15 is a junction in Figure 2a and then becomes a terminal point in Figure 2c. EU 5 is also a junction in Figure 2a and then turns to be a divalent point in Figure 2b. Also note that there exist two bridges between EU 15 and EU 17 in Figure 2c. Finally, it is found that the EEJP is EU 17 only.

Example 2. Figure 3 illustrates an example of deleting the EUs that have two independent paths to the INF network through EU 7 and EU 9. The original structure in Figure 3a contains no terminals. Thus, when running the above procedure, Step 1 is skipped. By executing Step 2, those divalent points (EU 1–EU 6), the junction (EU 10), and the associated bridges are all deleted, and a bridge between EU 7 and EU 9 is established. Moreover, EU 8 and EU 11 and their bridges to EU 7 are also replaced by new bridges directly. In this process, EU 10 is a junction in Figure 3a, but then becomes a divalent point and thus is also replaced by a new bridge. Also note that EU 1 and EU 10 in Figure 3a are a divalent point and a junction, respectively. Each of the two EUs has two independent paths to the INF network (through EU 7 and EU 9); they are all eliminated in Figure 3b. Finally, the EEJPs are EU 7 and EU 9, and their connection is also identified.

Determination of the number of elastically effective network chains

The reduced network consists of a number of EEJPs and the bridges connecting them. The bridges are network chains. A network chain is elastically effective only when it is long and its ends are EEJPs.[18] Thus, all short chains (i.e., short bridges) should be deleted. Note that a chain can link (i) two cross-linkers, (ii) a cross-linker and an effective monomer, (iii) two effective monomers that are initially in two different precursor polymer chains, or (iv) two effective monomers that are initially in the same precursor polymer chain. Because the fourth type of chains is short, only the first three types of chains need to be included in N_{EENC}, which can be counted as follows:

Step 1. Set the EENC counter to 0.

Step 2. Check all nonzero elements in matrix $\boldsymbol{G}$ sequentially. If an element (e.g., it has a value of j) is in the i-th row of $\boldsymbol{G}$, and the i-th and the j-th EUs are not effective monomers that are initially in the same precursor polymer chain, then the EENC counter is increased by 1. This step proceeds until all the nonzero elements in matrix $\boldsymbol{G}$ have been checked.

Step 3. As a chain has two ends, the value of the EENC counter divided by two gives N_{EENC}.

Coating quality evaluation

The time series data of $N_{\mathrm{EENC}}(t)$ and $N_{\mathrm{b}}(t)$ obtained from the LMC simulation are essential for calculating EECD(t). Note that the coating quality is reflected by EECD(t_{end}) which is the value when the curing process is terminated. Nevertheless, the trajectory of EECD(t) during the entire curing operation is also extremely important, as it can provide critical information of coating quality development. This may suggest a better curing strategy for more desirable baking and also possibly more energy efficient baking. On the other hand, this information also provides opportunities for performing a trade-off between coating quality, processing performance and cost.

According to Bauer and Dickie, a very small EECD indicates that the coating is underbaked and thus tends to be sensitive to humidity and solvent. On the other hand, a very large EECD is a sign of an overly baked coating, which means a typical intercoat adhesion failure in the coating.[16] The most desirable value range of the EECD is dependent on the type of paint material. This information should be provided by paint designers. For the acrylic-melamine paint based coating, for instance, it was found that the optimal value is 1.0×10^{-3} mol/g, with its desirable range between 0.8×10^{-3} mol/g and 1.25×10^{-3} mol/g.[17]

Case Study on Automotive Paint

The introduced modeling and simulation methodology has been successfully employed to study the acrylic-melamine resin-based paint for automotive coating manufacturing. In this section, we study the coating quality for a base case resin design first. Then, we investigate in depth how the number average molecular weight will affect coating quality. After that, we will show the initial results of the paint formulation design. Comparisons will be given to show the efficacy of the introduced methodology.

Material specification

The material of interest is the acrylic-melamine resin, a representative paint material widely used in the automotive industry. The polymer is a hydroxyl-functional acrylic copolymer, whose number average molecular weight ($\overline{M}_{\mathrm{n}}$) can be selected in the range from 1000 g/mol to 6000 g/mol. The molecular weight of an effective monomer (M_{m}) is 360 g/mol. The cross-linker is hexamethoxy-methylmelamine (HMMM), with the molecular weight of 390 g/mol and the functionality of 6. The hydroxy equivalent weight of the resin ($M_{\mathrm{A}}^{\mathrm{eq}}$) is 650 g/mol and the volume fraction of the resin in the paint (ϕ) is around 45%. The number ratio of the

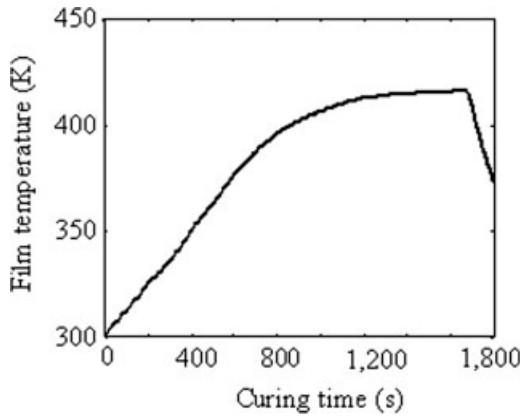

Figure 5. Imposed nonisothermal curing condition for paint formulation design.

methoxy group of the HMMM to the hydroxy group of the precursor polymer chains (r_{BA}) can be selected in the range from 0.95 to 2.5. There is primarily one type of cross-linking reaction in this system. As shown in Figure 4, the hydroxy group (i.e., Type A functional group) reacts with the methoxy group (i.e., Type B functional group) to form cross-links, where the methanol is generated as a byproduct. For this first order reaction, the frequency factor is 1.11×10^4 s^{-1} and the activation energy is 5.23×10^4 J/mol.[17]

Base curing case

In automotive coating development, paint is applied to the vehicle surface to generate a very thin layer of film. This wet film is then cured under a nonisothermal condition (see a representative curing temperature profile in Figure 5).[29] This coating development operation is very different from the lab-based isothermal curing during material development. For this base case, the number average molecular weight ($\overline{M}_n$) is 3000 g/mol, and the number ratio of the methoxy group of the HMMM to the hydroxy group of the precursor polymer chains (r_{BA}) is 1.5.

Simulation Set-Up. A lattice of $55 \times 55 \times 55$ cells is designed, where the volume fraction of polymer chains and cross-linkers in the system is 45%. The prespecified total number of the effective monomers (N_m^{set}) is set to 9000. By using Eqs. 3–6, a total of 1078 polymer chains (N_p) with 44 different lengths are generated; the total number of effective monomers (N_m) in the simulation is 8853. In this case, the number of polymer chains having a length beyond 44 calculated by Eq. 3 is always 0. Figure 6a shows the most probable molecular weight distribution of the polymer, where each circle gives a weight fraction of the polymer chains with a specific molecular weight (or length, or the number of effective monomers on it). Note that some circles deviate slightly from the curve; this is because the number of polymer chains of any specific length should be an integer in simulation, according to Eq. 3.

The number of hydroxy groups randomly distributed in the polymer chain (N_A^0) and the number of cross-linker molecules (N_c) are evaluated using Eqs. 8 and 10, respectively; the results are given in Table 1. For this base case ($\overline{M}_n$ and r_{BA} are 3000 g/mol and 1.5, respectively), the total number of the hydroxy groups in the polymer chains is 5952. The group distribution is shown in Figure 6b, where each triangle indicates a cumulative weight fraction of the polymer chains that have a specific number of the hydroxy groups. For instance, the figure shows that 9.7% of the polymer chains have none, one, and two hydroxy groups, and for any chain, the maximum number of hydroxy groups is 29.

Initial Configuration and Equilibrium State. The initial system structure is shown in Figure 7a. This and all other 3D structures are plotted using the visual molecular dynamics (VMD) software.[30] In the figure, the green and the red spheres represent the effective monomers and the cross-linkers, respectively. The bonds connecting the EUs are displayed as cylindrical rods. It is found that 553 bonds (out of 7775) cross the simulation lattice boundary due to the imposed PBC. These bonds are not shown explicitly and the effective monomers connected by these bonds are shown by the blue spheres in the figure.

The initial system that contains 10,341 EUs (including 8853 effective monomers and 1488 cross-linkers) takes

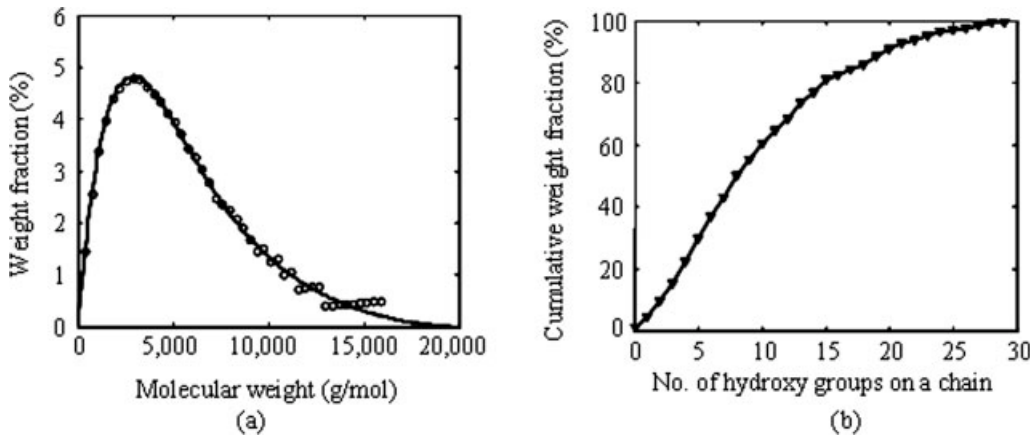

Figure 6. Information for the resin of the base case material: (a) the molecular weight distribution of polymer chains and (b) the functional groups distribution.

Table 1. Lattice MC Simulation Parameters for Different Materials

	$\overline{M}_n$ = 1000 g/mol					
Parameters	r_{BA} = 0.95	r_{BA} = 1.0	r_{BA} = 1.2	r_{BA} = 1.5	r_{BA} = 2.0	r_{BA} = 2.5
Polymer						
N_m	8987	8987	8987	8987	8987	8987
N_p	3239	3239	3239	3239	3239	3239
N_A^0	5664	5696	5829	6042	6432	6865
Crosslinker						
N_c	897	949	1166	1511	2144	2865
	$\overline{M}_n$ = 2000 g/mol					
Parameters	r_{BA} = 0.95	r_{BA} = 1.0	r_{BA} = 1.2	r_{BA} = 1.5	r_{BA} = 2.0	r_{BA} = 2.5
Polymer						
N_m	8967	8967	8967	8967	8967	8967
N_p	1621	1621	1621	1621	1621	1621
N_A^0	5651	5683	5816	6028	6418	6861
Crosslinker						
N_c	895	947	1163	1507	2139	2859
	$\overline{M}_n$ = 3000 g/mol					
Parameters	r_{BA} = 0.95	r_{BA} = 1.0	r_{BA} = 1.2	r_{BA} = 1.5	r_{BA} = 2.0	r_{BA} = 2.5
Polymer						
N_m	8853	8853	8853	8853	8853	8853
N_p	1078	1078	1078	1078	1078	1078
N_A^0	5579	5611	5742	5952	6336	6774
Crosslinker						
N_c	883	935	1148	1488	2112	2823
	$\overline{M}_n$ = 4000 g/mol					
Parameters	r_{BA} = 0.95	r_{BA} = 1.0	r_{BA} = 1.2	r_{BA} = 1.5	r_{BA} = 2.0	r_{BA} = 2.5
Polymer						
N_m	8718	8718	8718	8718	8718	8718
N_p	804	804	804	804	804	804
N_A^0	5494	5525	5655	5861	6240	6671
Crosslinker						
N_c	870	921	1131	1465	2080	2780
	$\overline{M}_n$ = 5 000 g/mol					
Parameters	r_{BA} = 0.95	r_{BA} = 1.0	r_{BA} = 1.2	r_{BA} = 1.5	r_{BA} = 2.0	r_{BA} = 2.5
Polymer						
N_m	8633	8633	8633	8633	8633	8633
N_p	644	644	644	644	644	644
N_A^0	5440	5472	5600	5804	6179	6605
Crosslinker						
N_c	861	912	1120	1451	2060	2752
	$\overline{M}_n$ = 6000 g/mol					
Parameters	r_{BA} = 0.95	r_{BA} = 1.0	r_{BA} = 1.2	r_{BA} = 1.5	r_{BA} = 2.0	r_{BA} = 2.5
Polymer						
N_m	8414	8414	8414	8414	8414	8414
N_p	531	531	531	531	531	531
N_A^0	5302	5333	5458	5656	6022	6438
Crosslinker						
N_c	839	889	1092	1414	2007	2683

around 10^9 MC steps to reach the equilibrium state. A microstructure of the system at the equilibrium state is shown in Figure 7b.

Coating Curing. According to the usual industrial practice, the curing time is set to 30 min, which is equivalent to 14,156,829 MC steps, according to the calculation by following the MC step-curing time conversion procedure that was introduced earlier.

Coating microstructure. Figure 7c shows the coating microstructure at the end of the 30-min curing. In this struc-

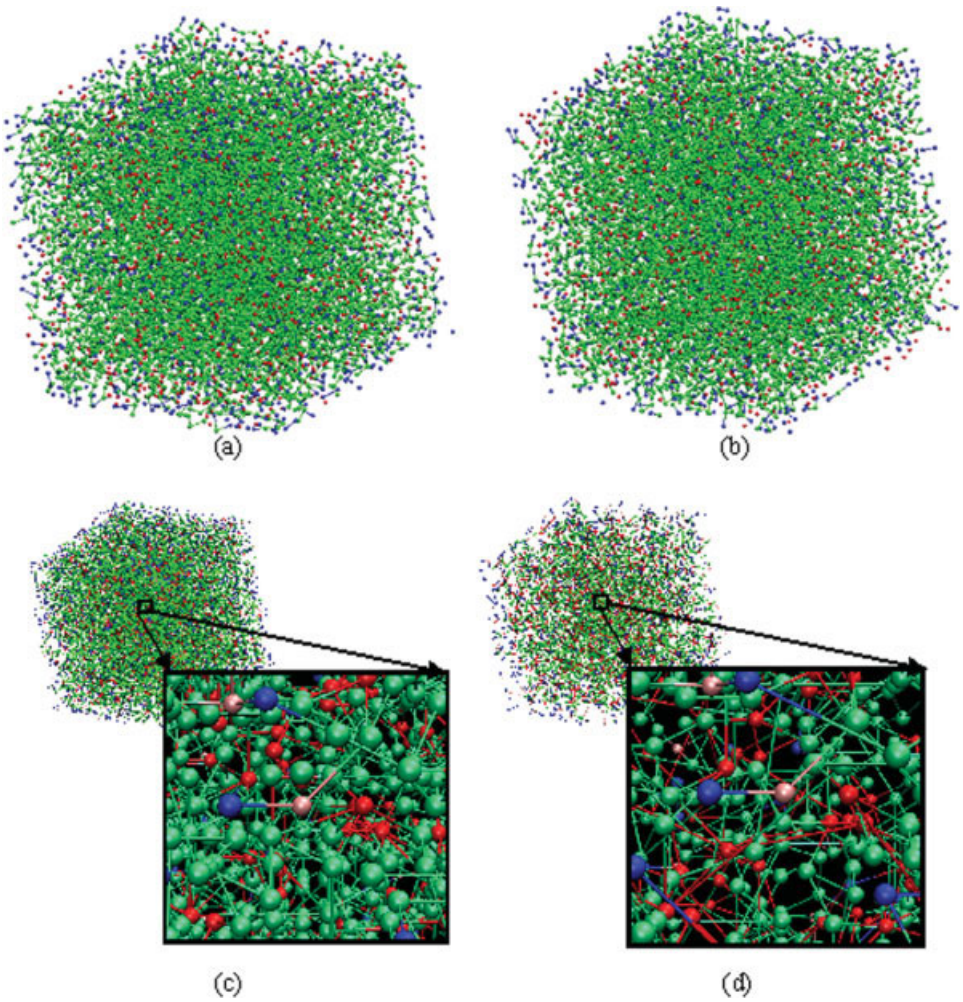

Figure 7. Coating microstructures (green and blue spheres: effective monomers; red and pink spheres: cross-linkers; cylindrical rods connecting spheres: bonds or bridges): (a) the initial structure, (b) the structure at the equilibrium state, (c) the structure at the end of curing with a close-up view, and (d) the reduced network with a close-up view.

[Color figure can be viewed in the online issue, which is available at www.interscience.wiley.com.]

ture, there are 5539 bonds newly created from the cross-linking reaction. These bonds connect effective monomers and cross-linkers (see the cylindrical rods between the green and the red spheres in a close-up view of Figure 7c), which are different from the other bonds that are between the effective monomers (see Figures 7a, b). Note that some cross-linkers are connected to the EUs beyond the lattice boundary (see the pink spheres in Figure 7c). After identifying the network and the EEJPs and their connections contained in the structure in Figure 7c, a reduced network is generated that is shown in Figure 7d. In this structure, each EU connects to at least three other EUs (see a close-up view of the figure). This reduced network is used for EECD calculation.

Gel point identification. The gel point formation in the system can be revealed through plotting the relationship between the conversion and the reduced weight average molecular weight of the system (i.e., the weight average molecular weight of the system excluding the largest molecule).[31] In this study, the gel point appears when the conversion reaches 30% (see Figure 8a). Note that after the gel point, the network of infinite size starts to form and the EECD starts to increase from 0 (see Figure 8b).

The EECD dynamics obtained from the M&M theory is plotted in Figure 8b (see the dashed curve), which shows the gel point occurring at the conversion of 21.9%. The comparison indicates that the M&M theory underestimates the gel point; the reason for this needs a further investigation.

Curing dynamics. As shown in Figure 9a, in the early stage of curing (the first ~400 s), the reaction takes place slowly so as the conversion because the film temperature is relatively low. As the curing temperature increases (see the heating profile in Figure 5), the film temperature will be raised, which accelerates the reaction. But then this becomes slower, as it reaches a high conversion (i.e., after 1600 s of curing).

It is interesting to note that the conversion dynamics along the MC steps is very different from that along curing time. As shown in Figure 9b, the conversion takes off very quickly

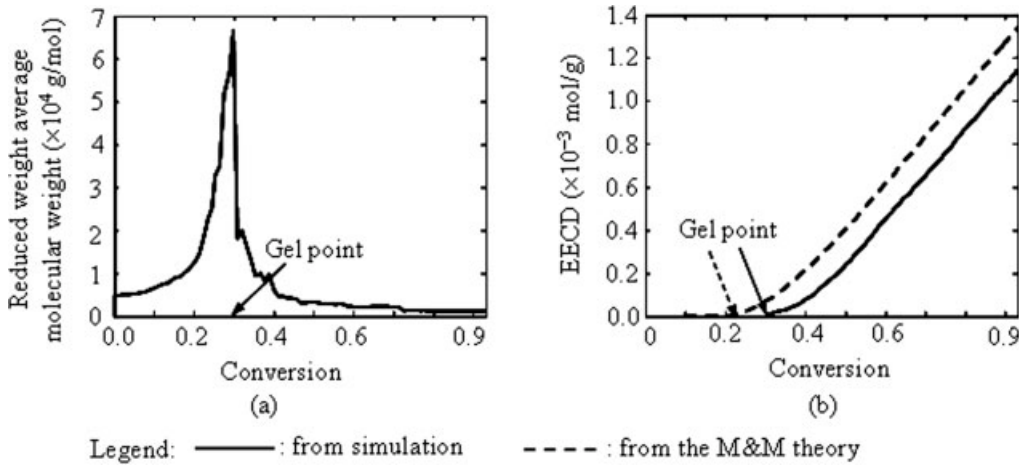

Figure 8. Gel point prediction and comparison.

within the first $\sim 10^6$ MC steps, and then it slows down during the rest 13×10^6 steps. This can be readily understood by the fact that in an athermal approach,[5,13] the reaction speed depends on the availability of not reacted functional groups and the mobility of polymer chains and cross-linkers, which are continuously decreased along the MC steps.

The comparison of the conversion dynamics indicates clearly that the number of MC steps passed is not proportional to the curing time elapsed, which disproves a claim of a proportional relationship between the MC steps and the time made by Gina et al.[13] As shown in Figures 9a, b, when the conversion reaches 40%, for example, $\sim 2.79 \times 10^5$ MC steps are finished in simulation, which is equivalent to $\sim$934 s of curing time. For the conversion doubled to 80%, it needs to take $\sim 3.79 \times 10^6$ new MC steps, which is equivalent to $\sim$454 s.

Coating Quality Evaluation. As stated, coating quality is assessed by the information of the EECD. For this reason, the EECD dynamics along the curing time and that along the MC steps are plotted in Figures 9c,d, respectively. As shown,

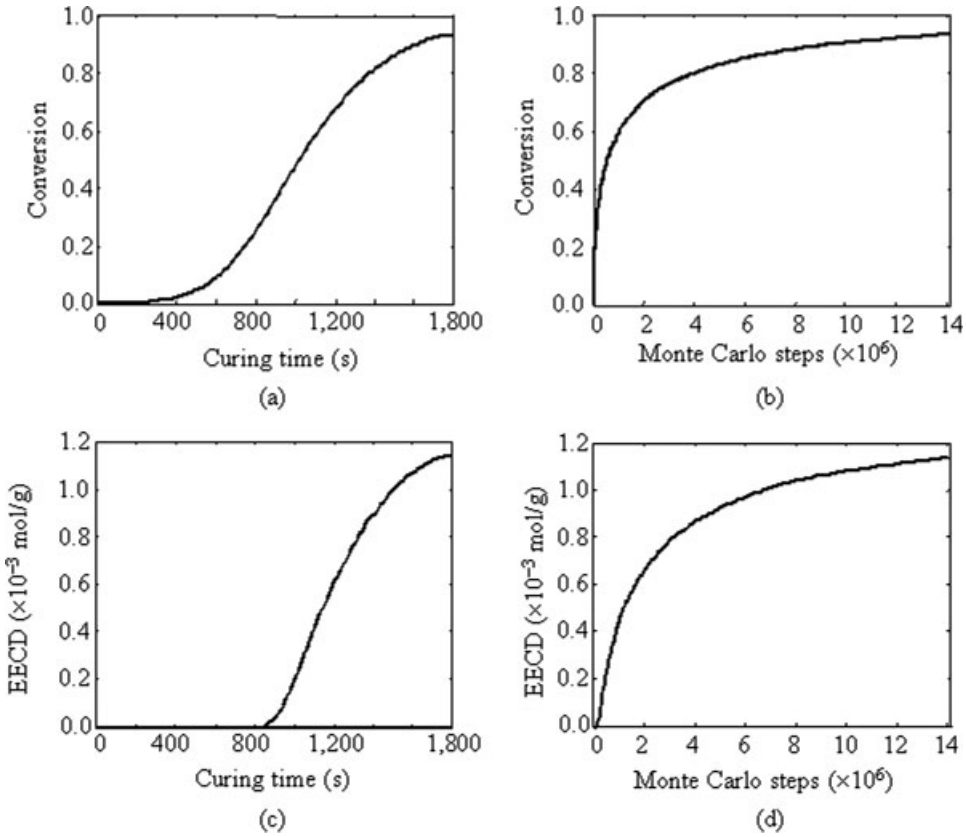

Figure 9. Curing dynamics.

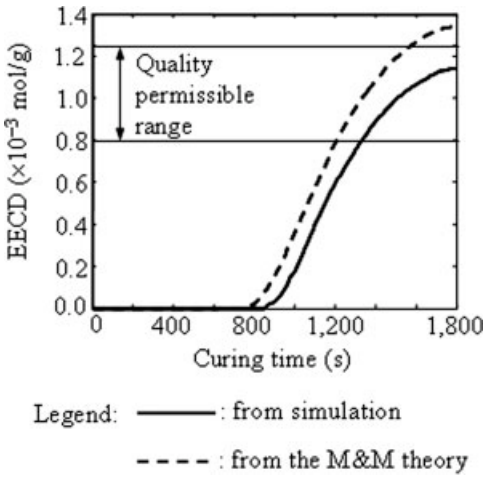

Figure 10. EECD dynamics.

at the end of the 30-min curing, the EECD reaches 1.14×10^{-3} mol/g, which indicates a superior coating quality (for the desirable EECD range of 0.8×10^{-3} to 1.25×10^{-3} mol/g). Correspondingly, the hydroxy group conversion reaches 93%.

In Figure 10, the EECD dynamics is compared with the result (see the dashed curve) provided by Bauer et al., which was obtained based on the M&M theory.[15,18,19] It is shown that the M&M theory overestimates the EECD in this case. This overestimation is caused by an ignorance of loops and miscounting of pendent materials; such an EECD estimation may generate an erroneous interpretation of the coating quality problems. For example, the EECD value of 1.34×10^{-3} mol/g by Bauer et al. considered the film which was already overly baked. However, this is not true, because the EECD should be 1.14×10^{-3} mol/g which is close to the most desirable value (1.0×10^{-3} mol/g).

Computational Time. In this work, the simulations were conducted on one compute node (Xeon dual processor node @2.66 GHz) of an Aspen Beowulf Cluster system. The computational time for the base case is ~33.5 min, among which ~98.5% of the time is used for the equilibrium state creation. The other 1.5% is for coating curing and quality evaluation. The computational time for the system set-up and initial configuration generation is nearly negligible. As no report on the computational time has been identified for the LMC-based polymer network simulations,[5,10–14] a direct comparison of the computational efficiency of the introduced method with others cannot be made.

Effect of the number average molecular weight

The number average molecular weight ($\overline{M}_n$) is one of the key parameters that influences curing dynamics and coating quality. In this work, three different $\overline{M}_n$'s (1000, 3000, and 5000 g/mol) with the same functional groups ratio (r_{BA}) of 1.5 are studied, each of which is cured under the same curing condition shown in Figure 5. The three resins have different parameters (i.e., N_m, N_p, N_A^0, and N_c), which are listed in Table 1.

Molecular Weight and Functional Group Distribution. Figure 11 shows the distributions of the molecular weight and the functional groups for the polymers. It is found that if $\overline{M}_n$ is smaller, then a higher weight fraction will be given to the shorter polymer chains (i.e., with lower molecular weights) (see Figure 11a). Also, the curve of the cumulative weight fraction of polymer chains shifts to the left, which means that more chains have less functional groups (see Figure 11b).

Cross-linking Conversion, EECD Dynamics, and Coating Quality. It is shown that when the 30-min curing process ends, all the three coatings achieve the same conversion of 93% (see Figure 12a), but the EECD values are quite different (see Figure 12b). It shows that the only satisfactory coating is the one with $\overline{M}_n$ of 3000 g/mol, as its EECD value is within the permissible range. The other two are either slightly overbaked (for $\overline{M}_n$ of 5000 g/mol) or clearly underbaked (for $\overline{M}_n$ of 1000 g/mol).

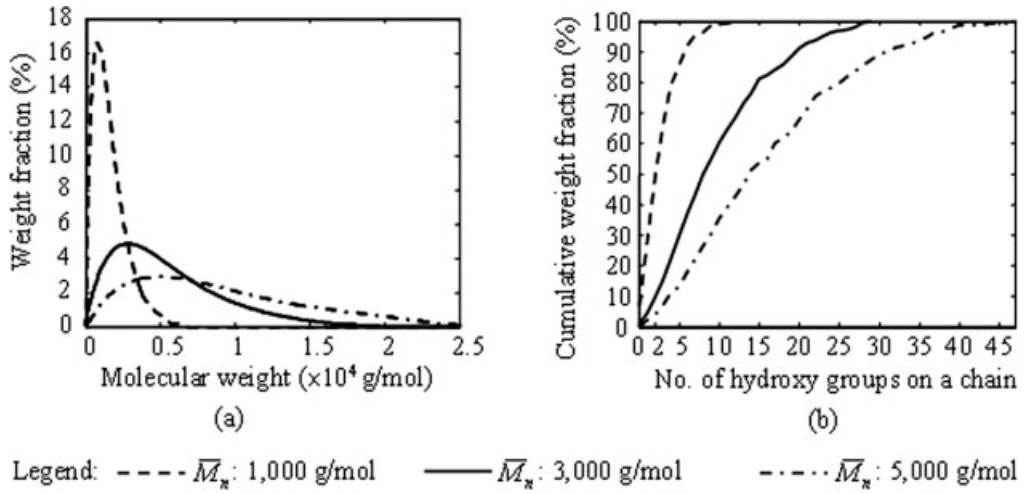

Figure 11. Distributions of molecular weights and functional groups in the three resins.

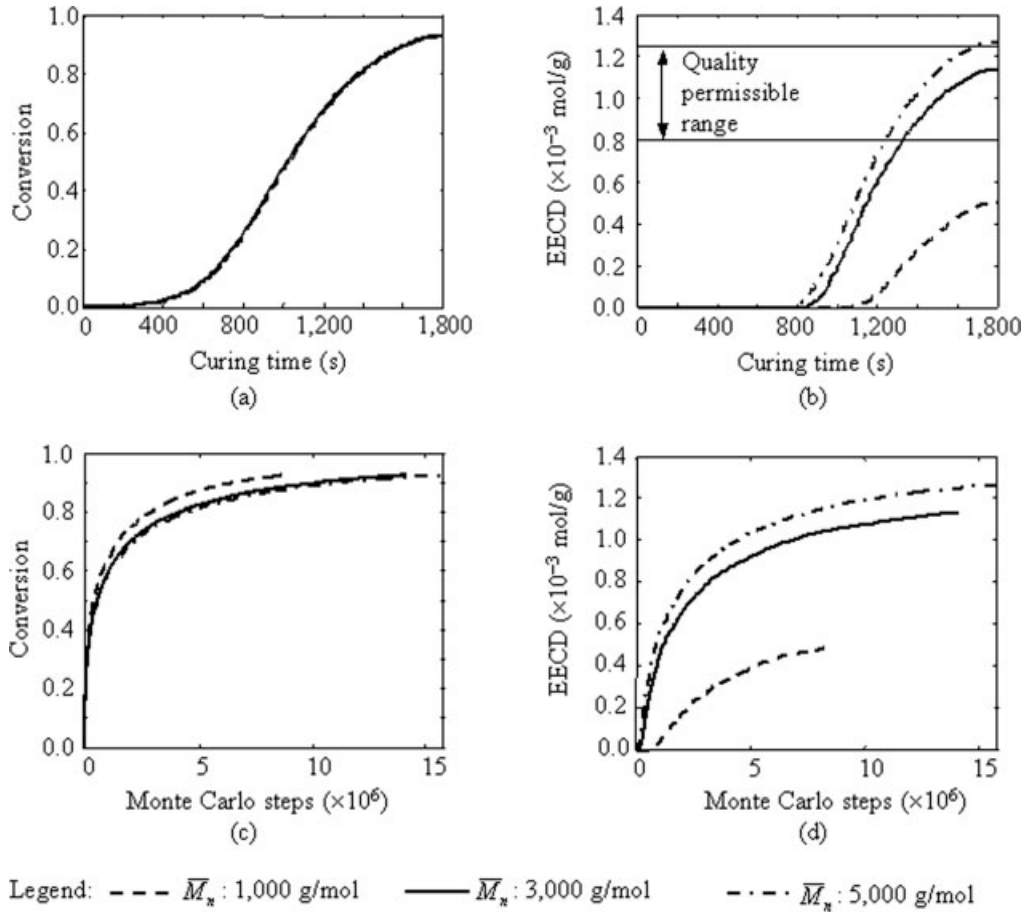

Figure 12. Curing dynamics along time and Monte Carlo step for the three coatings.

The simulation shows that for the coatings achieving the same conversion, the smaller the $\overline{M}_n$ value of a polymer, the smaller the EECD value. This finding is consistent with the experimental results.[15–17] This can be attributed to two reasons. First, the chance for the shorter chains to form loops is much greater than that for the longer chains. The formed loops must be eliminated or replaced by bridges when generating the reduced network from the INF network, which is the basis of EECD evaluation. Second, the polymer chains with two or less functional groups cannot form elastically effective junctions.[15] As shown in Figure 11b, the cumulative weight fractions of the polymer chains with no more than two functional groups in the coatings with the $\overline{M}_n$ values of 1000 g/mol, 3000 g/mol, and 5000 g/mol are 50%, 9.7%, and 4%, respectively. This significant difference of the cumulative weight fractions causes a major difference of the final EECD values (see Figure 12b).

The conversion and the EECD evolutions along the MC steps of the three polymer materials are plotted in Figures 12c, d. It is interesting to note that for the same curing time of 30 min, the simulations for the three coatings are stopped in different MC steps. It is observed that a lower $\overline{M}_n$ polymer has fast reactions in each MC step; thus, the total number of MC steps is less than that for a higher $\overline{M}_n$ polymer. This is different from the conversion dynamics in the time domain that has no difference for the materials with different $\overline{M}_n$'s (see Figure 12a).

Comparison with the M&M Theory Prediction. As a comparison, the EECD and the gel point based on the M&M theory are also studied. It is found that the M&M theory-based approach overestimated the EECD (see Figure 13a and also Table 2), but underestimated the occurrence of the gel point (see Figure 13b). Obviously, the overestimation of the EECD gives erroneous conclusion on coating quality. A fundamental reason of the overestimation is due to the ignorance of the loop formation and miscounting the pendent material. Note that a resin with a lower $\overline{M}_n$ has more chains of shorter lengths and less functional groups, and thus is more likely to form loops and pendent materials.

EECD-focused paint material design

To identify a superior paint formulation, the effect of the number average molecular weight ($\overline{M}_n$) and the functional groups ratio (r_{BA}) on coating quality must be thoroughly investigated. In this study, a total of 36 coatings with six different $\overline{M}_n$'s in the range of 1000–6000 g/mol and six different r_{BA}'s in the range of 0.95–2.5 are individually cured to the same conversion. Table 1 lists the material parameters for all 36 coatings. To ensure prediction reliability, four inde-

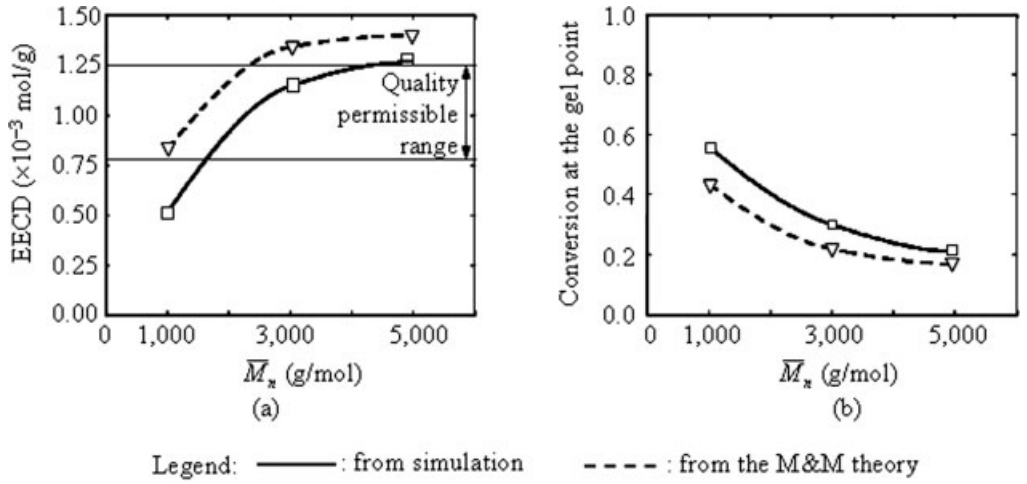

Figure 13. Identification of the final EECD and the gel point for the three coatings cured under the same condition.

pendent simulation runs are conducted for each coating system, which can generate an averaged EECD for comparison. Thus, a total of 144 (36 × 4) simulations are needed to have a thorough investigation of the design space and to provide an excellent guideline for formulation selection.

Formulation Identification. In the first set of simulations, each of the 36 coatings is cured to 90% conversion, at which the average EECD values are depicted in Figure 14 (see the 36 black dots). A 3D response surface is generated based on these 36 values. Note that error bars are omitted in the figure because the standard deviations of EECD values are very small ($<0.02 \times 10^{-3}$ mol/g). It is shown that for the coatings with the same r_{BA}, the EECD will be increased along $\overline{M}_n$. However, when $\overline{M}_n$ is fixed, the EECD is increased when r_{BA} is decreased.

The 3D surface can facilitate greatly paint formulation selection. For the resin made by the hydroxyl-functional acrylic copolymer and the HMMM cross-linkers, it was found that the EECD should be within the range from 0.8×10^{-3} mol/g to 1.25×10^{-3} mol/g, with the optimal value of 1.0×10^{-3} mol/g.[17] In Figure 14, the lower and upper limits and the optimal value of EECD are plotted as three curves. For instance, if r_{BA} equals to 1, $\overline{M}_n$ can be chosen in the range between 1500 g/mol and 4400 g/mol, with 2000 g/mol as the optimal. By following the curve for the EECD at 1.0×10^{-3} mol/g, all optimal combinations of $\overline{M}_n$ and r_{BA} can be readily identified, which are the most desirable design of paint formulations.

As a very large and critical part of the design space for paint formulations was explored, it is believed that the physics of the network systems useful for paint formulation selection was sufficiently captured. On the other hand, the identified superior formulations are highly desirable because of the two reasons. First, the selected 36 coating systems were distributed widely throughout the entire design space and the stochastic errors were effectively reduced through conducting four simulation runs for each system. Second, the response surface is very smooth (see Figure 14), which indicates the reliability of the predictions.

Quality Assured Process Performance Improvement. The introduced methodology can not only guide optimal paint formulation design for ensured coating quality, but also help identify the opportunities for process performance improvement during material design. In the second set of simulations, all 36 coatings are cured to the conversion of 85%. The simulations allow identification of the optimal $\overline{M}_n - r_{BA}$ pairs for achieving the optimal EECD of 1.0×10^{-3} mol/g. This result is plotted in Figure 15. To make the comparison easy, the optimal EECD for the conversion of 90% that is already

Table 2. Comparison of EECD Prediction

Materials	EECD ($\times 10^{-3}$ mol/g) (from Simulation)	EECD ($\times 10^{-3}$ mol/g) (Based on the M&M Theory)	Difference (%)
$\overline{M}_n$ = 5000 g/mol	1.261	1.3976	10.83
$\overline{M}_n$ = 3000 g/mol	1.138	1.3397	17.72
$\overline{M}_n$ = 1000 g/mol	0.501	0.8279	65.25

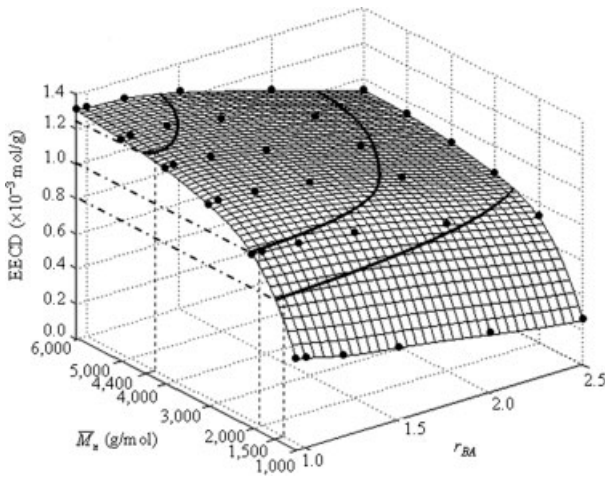

Figure 14. EECD correlation with $\overline{M}_n$ and r_{BA} for the coatings all cured to the same conversion of 90%.

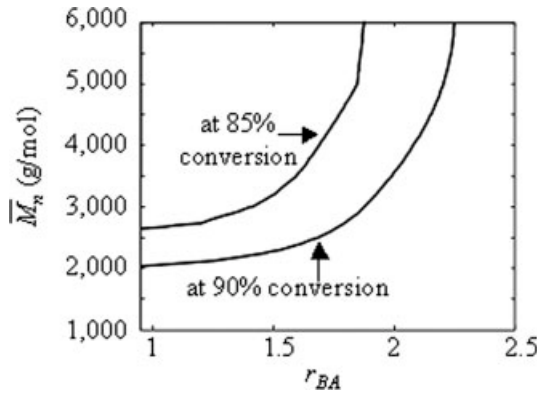

Figure 15. Optimal EECD correlation with $\overline{M}_n$ and r_{BA} for the coatings cured to different conversions.

shown in the surface plane of Figure 14 is also plotted in Figure 15.

As a note, the introduced methodology allows the generation of any number of optimal EECD curves like those in Figure 15, as long as a preferred conversion is given. The curves can provide an optimal selection of $\overline{M}_n$ and r_{BA} for achieving a lower cross-linking conversion percentage, which means lower energy consumption. As shown in the figure, a resin containing a greater $\overline{M}_n$ polymer can help reduce energy consumption when the coating is baked in oven. This has been confirmed experimentally.[15–17] But if the paint is solvent borne, then a resin containing a lower $\overline{M}_n$ polymer will be preferred because it will require a less amount of solvent (i.e., less VOC emission). Therefore, if reliable energy and emission models are available, then the correlation among $\overline{M}_n$, r_{BA}, and EECD can be appropriately established. Paint designers can then use it to perform a trade-off among coating quality, energy efficiency, and environmental cleanness.

Conclusions

How to improve paint formulation design is becoming a focal point in ensuring a full realization of anticipated coating properties, introducing new coating properties, and improving paint application efficiencies. In this work, a systematic paint formulation design methodology is introduced by resorting to LMC modeling and simulation techniques. By this methodology, a variety of quantitative correlations among paint material, curing condition, coating microstructure, and coating qualities can be established. The formulation of paint, with a focus on its resin, can be optimally designed based on the identified correlations.

The unique features of the methodology are threefolds. First, this is among the earliest to use LMC with a BF model to study paint material design. The 3D simulations by this methodology can generate the critical information needed by paint designers to improve their experimental design and to have more comprehensive and deep understandings of how a paint formulation selection can influence coating property, energy efficiency, and possibly VOC emission. Second, this is mostly the first time to impose practical curing conditions to investigate polymeric network formation during paint-based coating curing. This allows the study of curing dynamics under interested curing conditions along both the MC steps and the real operational time. Third, this is again among the earliest efforts to extract and utilize the information contained in 3D polymeric network structures to study a critical coating quality indicator. This can help greatly bridge the gap between the research on microscale paint material structures and the investigation on macroscopic coating quality. A comprehensive study on acrylic-melamine-based paint design and analysis has demonstrated the efficacy of the introduced methodology.

The developed methodology can be employed to deepen the study on optimal paint design in a larger scope in the future. Although the current investigation is on a specific type of resin in paint, the methodology can be readily applied to other types of resins and also be extendable to the studies on the paint with other components, such as solvent, pigment and additive. Undoubtedly, more comprehensive studies on material structure-coating property correlations should be conducted. Other structural parameters quantifiable from 3D networks are expected to be identified for correlating with additional coating properties. Furthermore, the issues of energy, environment, and product life cycle can be addressed in paint formula design. Needless to say, all the correlation and paint design improvement strategies identified through simulation must be experimentally validated by paint designers and end users. All these tasks are very challenging and require collaborative efforts among experimental and computational paint designers and end users.

Acknowledgments

This work is supported in part by NSF (CMMI 0700178), and the Institute of Manufacturing Research and the Thomas Rumble Fellowship Program of Wayne State University. The authors also wish to gratefully acknowledge the editor and reviewers' constructive comments on the earlier versions of this article.

Notation

$\boldsymbol{B}$ = bond matrix
$\boldsymbol{D}$ = molecule index vector
EECD = elastically effective cross-link density (mol/g)
$\boldsymbol{F}$ = EU functionality vector
$\boldsymbol{G}$ = EU connection matrix
$\boldsymbol{L}$ = lattice cell occupation matrix
M_c = molecular weight of a cross-linker molecule (g/mol)
M_m = molecular weight of an effective monomer (g/mol)
$\overline{M}_n$ = number average molecular weight of the polymer (g/mol)
N_c = number of cross-linkers
N_{EENC} = number of elastically effective network chains
N_m = number of effective monomers in the simulation
N_p = number of precursor polymer chains
r_{BA} = ratio of the number of Type B to that of Type A functional groups
t = curing time (s)
T = curing temperature (K)
$\boldsymbol{U}$ = EU location matrix
α = cross-linking reaction conversion
ϕ = volume fraction of polymer chains and cross-linkers
ω = a bond vector
Ω = the set of permissible bond vectors

Literature Cited

1. Xiao J, Li J, Lou HH, Huang YL. Cure-window-based proactive quality control in topcoat curing. *Ind Eng Chem Res*. 2006;45:2351–2360.
2. Xiao J, Li J, Lou HH, Xu Q, Huang YL. ACS-based dynamic optimization for curing of polymeric coating. *AIChE J*. 2006;52:1410–1422.
3. Li J, Xiao J, Huang YL, Lou HH. Integrated process and product analysis: a multiscale approach to paint spray. *AIChE J*. 2007;53: 2841–2857.
4. Schoff CK. Organic coatings: the paradoxical material. *Prog Organic Coat*. 2005;52:21–27.
5. Balabanyan AG, Kramarenko EY, Ronova IA, Khokhlov AR. Monte Carlo study of structure and kinetics of formation of end-linked polymer networks. *Polymer*. 2005;46:4248–4257.
6. Cheng KC, Chiu WY. Monte Carlo simulation of polymer network formation with complex chemical reaction mechanism: kinetic approach on curing of epoxides with amines. *Macromolecules*. 1994; 27:3406–3414.
7. Tobita H. Simulation model for the modification of polymers via crosslinking and degradation. *Polymer*. 1995;36:2585–2596.
8. Yan LT, Qian ZY, Guo BH, Xu J, Xie XM. Monte Carlo simulation of chain extension using bisoxazolines as coupling agent. *Polymer*. 2005;46:11918–11926.
9. Johnston RT. Crosslinking simulations in polymer design. In: Galiatsatos V, editor. *Molecular Simulation Methods for Predicting Polymer Properties*. NJ: Wiley, 2005. pp. 243–275.
10. Schulz M, Sommer JU. Monte Carlo studies of polymer network formation. *J Chem Phys*. 1992;96:7102–7107.
11. Trautenberg HL, Sommer JU, Goritz D. Structure and swelling of end-linked model networks. *J Chem Soc Faraday Trans*. 1995;91: 2649–2653.
12. Hagn C, Wittkop M, Kreitmeier S, Trautenberg HL, Holzl T, Goritz D. The creation and spatial structure of end-linked bimodal polymer networks: a Monte Carlo study. *Polym Gels Networks*. 1995;5:327–337.
13. Gina N, Cohen C, Panagiotopoulos AZ. A Monte Carlo study of the structural properties of end-linked polymer networks. *J Chem Phys*. 2000;112:6910–6916.
14. Michalke W, Lang M, Kreitmeier S, Goritz D. Simulation on the number of entanglements of polymer network using knot theory. *Phys Rev E*. 2001;64:012801–1-4.
15. Bauer DR, Budde GF. Cross-linking chemistry and network structure in high solids acrylic-melamine coatings. *Ind Eng Chem Prod Res Dev*. 1981;20:674–679.
16. Bauer DR, Dickie RA. Cure response in acrylic copolymer/melamine formaldehyde crosslinked coatings. *J Coat Technol*. 1982;54:57.
17. Bauer DR, Dickie RA. Development and application of network structure models to optimization of bake conditions for thermoset coatings. *J Coat Technol*. 1986;58:41–48.
18. Miller DR, Macosko CW. A new derivation of post gel properties of network polymers. *Macromolecules*. 1976;9:206–211.
19. Macosko CW, Miller DR. A new derivation of average molecular weights of nonlinear polymers. *Macromolecules*. 1976;9:199–206.
20. Carmesin I, Kremer K. The bond fluctuation method: a new effective algorithm for the dynamics of polymers in all spatial dimensions. *Macromolecules*. 1988;21:2819–2823.
21. Deutsch HP, Binder K. Interdiffusion and self-diffusion in polymer mixtures: a Monte Carlo study. *J Chem Phys*. 1991;94:2294–2304.
22. Frenkel D, Smit B. *Understanding Molecular Simulation from Algorithms to Applications*. San Diego, CA: Academic Press, 2002.
23. Lamm MH, Chen T, Glotzer SC. Simulated assembly of nanostructured organic/inorganic networks. *Nano Lett*. 2003;3:989–994.
24. Flory PJ. *Principles of Polymer Chemistry*. Ithaca, NY: Cornell University Press, 1995.
25. Dickie RA, Bauer DR, Ward SM, Wagner DA. Modeling paint and adhesive cure in automotive applications. *Prog Organic Coat*. 1997;31:209–216.
26. Chen T, Lamm MH, Glotzer SC. Biomolecule-directed assembly of nanoscale building blocks studied via lattice Monte Carlo simulation. *J Chem Phys*. 2004;121:3919–3929.
27. Nijenhuis A, Wilf HS. *Combinatorial Algorithm*. New York: Academic Press, 1975.
28. Eichinger BE, Akgiray O. Computer simulation of polymer network formation. In: Colbourn EA, editor. *Computer Simulation of Polymers*. England: Longman Scientific and Technical, 1994. pp. 263–302.
29. Lou HH, Huang YL. Integrated modeling and simulation for improved reactive drying of clearcoat. *Ind Eng Chem Res*. 2000; 38:500–507.
30. Humphrey W, Dalke A, Schulten K. VMD—visual molecular dynamics. *J Mol Graph*. 1996;14:33–38.
31. Shy LY, Leung YK, Eichinger BE. Critical exponents for off-lattice gelation of polymer chains. *Macromolecules*. 1985;18:983–986.

Manuscript received Nov. 15, 2007, and revision received July 28, 2008.